

RESEARCH

Open Access



Tumor-associated macrophage-derived exosome miR-194 confers cisplatin resistance in GC cells

Yi Zhou¹, Yang-cheng Sun¹, Qiong-yan Zhang¹, Jing Wang¹, Xian-ya Zhu¹ and Xiang-yu Su^{2*}

Abstract

Objective At all stages of gastric cancer (GC), cisplatin is the first-line chemotherapeutic agent, but its efficacy remains limited, with a response rate of less than 20%, largely because of resistance to the drug. It aims to determine whether macrophage-derived exosomes are involved in the mechanism of cisplatin resistance, in order to identify potential methods for reversing resistance and improving patient outcomes.

Methods Macrophages induced by IL-13 and IL-4 were characterized using flow cytometry, then co-cultured with GC cells and cisplatin. Cell viability and apoptosis were subsequently evaluated through CCK-8 assays and flow cytometry. Exosome miR-194, derived from M2 macrophages, was characterized and co-cultured with gastric cancer cells and cisplatin to assess cell survival. Furthermore, a mouse GC model was established, and miR-194 was injected to observe tumor growth.

Results Results indicate that M2 macrophages enhance cisplatin resistance in gastric cancer cells mainly through miR-194, as demonstrated by CCK-8 and apoptosis assays. Cellular uptake experiments demonstrated that miR-194 can transfer from macrophages to GC cells and exert functional effects. Western blotting and PCR analysis further confirmed that macrophage-derived miR-194 inhibits apoptosis in GC cells and enhances cisplatin resistance by downregulating PTEN.

Conclusion Macrophage-derived miR-194 promotes cisplatin resistance in GC cells by inhibiting apoptosis through PTEN downregulation. These findings provide new insights and theoretical backing for clinical treatment strategies in GC.

Keywords Gastric cancer, miR-194, Macrophage, Cisplatin resistance, Apoptosis

Introduction

Incidence and mortality rates for gastric cancer (GC) remain high, despite its prevalence [1, 2]. In China, GC ranks second in mortality among malignant tumors [2].

In early-stage GC, there are no obvious symptoms, so most patients are detected at an advanced stage, when surgery isn't an option, making chemotherapy the main treatment option [3]. According to current treatment guidelines, platinum-based chemotherapeutic agents remain the cornerstone of chemotherapy for GC. Cisplatin (DDP), in particular, is a first-line drug for GC treatment across all stages [4]. However, the effectiveness of cisplatin alone or in combination with other drugs remains less than 20% [5]. Therefore, elucidating the mechanisms behind cisplatin resistance in GC cells, identifying ways to reverse this resistance, and improving

*Correspondence:

Xiang-yu Su
suxiangyu1982@163.com

¹ Department of Hematology and Oncology, Wuzhong People's Hospital, Suzhou 215000, China

² Department of Oncology, School of Medicine, Zhongda Hospital, Southeast University, Nanjing 210009, China



© The Author(s) 2025. **Open Access** This article is licensed under a Creative Commons Attribution-NonCommercial-NoDerivatives 4.0 International License, which permits any non-commercial use, sharing, distribution and reproduction in any medium or format, as long as you give appropriate credit to the original author(s) and the source, provide a link to the Creative Commons licence, and indicate if you modified the licensed material. You do not have permission under this licence to share adapted material derived from this article or parts of it. The images or other third party material in this article are included in the article's Creative Commons licence, unless indicated otherwise in a credit line to the material. If material is not included in the article's Creative Commons licence and your intended use is not permitted by statutory regulation or exceeds the permitted use, you will need to obtain permission directly from the copyright holder. To view a copy of this licence, visit <http://creativecommons.org/licenses/by-nc-nd/4.0/>.

patient prognosis and quality of life are urgent challenges in GC treatment [6].

Increasing evidence suggests that the occurrence and progression of tumors depend not only on the biological characteristics of the tumor cells themselves but also on the influence of the tumor microenvironment (TME) [7]. The TME encompasses not only tumor cells but also various non-malignant cells, such as inflammatory cells, fibroblasts, adipocytes, extracellular matrix, inflammatory mediators, and cytokines [8]. Tumor-associated macrophages (TAMs), integral to TME, significantly influence tumor progression [9]. Depending on the stimuli from cytokines or inflammatory factors, TAMs exhibit distinct phenotypes and functional characteristics [10]. Tumor cells or other cells within the TME can produce polarizing factors that induce TAMs to differentiate into either the classically activated macrophages (M1 subtype), which have antitumor effects, or alternatively activated macrophages (M2 subtype), which promote tumor progression [11]. In most malignancies, TAMs predominantly exhibit the M2 phenotype, further enhancing tumor malignancy, and tumor cells actively recruit macrophages and induce their polarization into the M2 subtype.

Exosomes are nano-sized extracellular vesicles (EVs) with a lipid bilayer membrane, produced and released by most cells [12]. Exosomes, present in all body fluids, have gained attention for their role in intercellular communication and potential as non-invasive tumor biomarkers [13]. Exosomes from tumor cells are involved in numerous cellular functions and pathological processes. Research indicates that plasma exosome protein levels in patients with various malignancies are significantly linked to disease activity, therapeutic response, and drug resistance.

In this study, we induced M2-polarized macrophages and analyzed their association with GC resistance [14]. We then examined the relationship between exosomes derived from M2 macrophages and cisplatin resistance in GC. Using confocal microscopy, we observed that miR-194 is transferred from M2 macrophage-derived exosomes to GC cells, reducing their chemosensitivity and apoptosis. Finally, we explored the mechanisms by which exosome miR-194 confers cisplatin resistance in GC, providing guidance for future research and potential clinical applications.

Materials and methods

Cell culture

The mouse forestomach carcinoma line MFC and human GC cell line MGC-803 were obtained from the Chinese Academy of Sciences Cell Bank. Cells were maintained in RPMI-1640 medium supplemented with 10% fetal

bovine serum and 100 U/mL penicillin–streptomycin. Cells were incubated at 37 °C in a humidified 5% CO₂ atmosphere. Annexin V-FITC, Cell Counting Kit-8, cisplatin, Annexin V-PE and 7-AAD were purchased from Beyotime Biotechnology. PBMCs were obtained from peripheral blood of volunteers in Suzhou Wuzhong people's Hospital, including 5 gastric cancer patients and 5 healthy volunteers, and were separated by density gradient centrifugation. To differentiate human monocytes into macrophages in vitro, monocytes were separated from PBMCs by negative selection using magnetic beads (Miltenyi Biotec), and the isolated cells were cultured in RPMI 1640 supplemented with 10% FBS (Gibco) for 7 days.

Flow cytometry

Exosomes from both MCF and MCF/DDP cells (50 µg/mL) were used to pre-stimulate cells for 72 h. Cisplatin (6 mg/mL) was then added for 48 h. Subsequently, cells were stained with Annexin V-PE and 7-AAD for apoptosis detection via flow cytometry (BD Biosciences), with PBS serving as the control.

Apoptosis detection

Cells were plated in six-well plates at a density of 10,000 cells/well. Apoptosis was assessed using the FITC Annexin V/PI Apoptosis Detection Kit. In summary, 5 µL each of Annexin V-FITC and propidium iodide were added to the wells and gently mixed. The treated cells were analyzed using a flow cytometer (BD Biosciences). The data were calculated and analyzed using Cell Quest software, and the apoptosis percentage for each group was determined.

Exosome isolation

Culture supernatants were collected upon cells reaching 80–90% confluence. The supernatant underwent a two-step centrifugation process [15]. In brief, the 48-h culture supernatant was collected and centrifuged at 3000×g for 20 min at 4 °C to remove cell debris. The supernatant was further centrifuged at 10,000×g for 60 min at 4 °C, followed by filtration through a sterile 0.22 µm microporous filter. Finally, the filtered supernatant was ultracentrifuged at 120,000×g for 70 min at 4 °C, and the resulting pellet was resuspended in an appropriate volume of PBS to obtain the exosomes, which were stored at –80 °C.

Cellular uptake of miR-194

To label MCF/DDP exosomes, 100 µL of exosomes were combined with 5 µL of Dil dye (5 µg/mL) in a new EP tube and mixed thoroughly. The pellet was resuspended in 200 µL of PBS after discarding the supernatant and then added to the MCF cell culture for 10–12 h. Cellular

uptake was observed and photographed using a laser confocal fluorescence microscope.

CCK-8 and crystal violet staining

GC cells were seeded in 96-well plates at a density of 1500–3000 cells/well and incubated with DDP for 24–72 h. Cell viability was assessed using the Cell Counting Kit-8 (CCK-8) according to the manufacturer's instructions. Absorbance was measured at 450 nm using a microplate reader (FLX800, Bio-TEK).

Transfected gastric cancer cells were seeded in 60 mm culture dishes at a density of 2×10^3 cells for colony formation assays. DDP was added to the culture medium at a final concentration of 5 μ M. After 1 or 2 days, the remaining colonies were fixed with 4% paraformaldehyde and stained with crystal violet.

MicroRNA microarray

Exosome pellets were collected from 10 mL of supernatant from M2-polarized macrophages and homogenized in Trizol (Invitrogen). Total RNA was quantified using a NanoDrop 2000c spectrophotometer (Thermo Scientific, USA) and its quality was assessed via capillary electrophoresis on an Agilent 2100 Bioanalyzer (Agilent Technologies, CA). miRNA microarray analysis was performed by Shanghai Biotechnology Corporation.

qT-PCR

Total RNA extraction was performed with Trizol (Invitrogen, USA) according to the manufacturer's guidelines. cDNA was synthesized using the Prime-Script RT reagent kit (Thermo Fisher, USA). Gene expression levels were quantified using quantitative polymerase chain reaction (qPCR) with the SYBR Green PCR kit (QIAGEN, Dusseldorf, Germany). β -actin served as the internal control. Target gene mRNA levels were normalized to β -actin using the $2^{-\Delta\Delta CT}$ method (Table 1).

Western blot (WB)

Protein samples of equal volume were analyzed using SDS-PAGE and transferred onto NC membranes. The

membranes were blocked with 5% skim milk in Tris-buffered saline, then incubated with primary antibodies (AKT, PTEN, Bcl-2, Rabbit, 1:1000) overnight at 4 °C, followed by a 2-h room temperature incubation with IRDye 800CW or 680 secondary antibodies (1:5000, LI-COR Biosciences, USA) on a rotating shaker. Signal detection was performed using ECL (GE, USA). Protein bands were imaged using a gel analysis system, and their grayscale values were analyzed with Image J software.

Animal experiments

Male C57 nude mice, aged 4–6 weeks, were obtained from the Shanghai Experimental Animal Center, China. Tumors were established in mice by subcutaneously injecting 300,000 cells. Ten days later, mice received intraperitoneal injections of 10 mg/kg cisplatin (DDP) or PBS. Before DDP treatment began, intratumoral injections of M2-Exos or miR-194 were administered twice. Tumor volume was measured every 2 days. Following treatment, the mice were euthanized to weigh the tumor masses. The Animal Research Ethics Committee of the Medical School approved all animal procedures.

Data analysis

Data were analyzed using SPSS version 21.0. Independent samples *t* tests were used for comparing two groups with normally distributed data and homogeneous variance, while one-way ANOVA was employed for comparisons among multiple groups. Dunnett's *t* test was employed for pairwise comparisons when the ANOVA indicated statistical significance. The Kruskal–Wallis *H* test, a non-parametric method, was used for data not suitable for ANOVA. Data were presented as mean \pm SD. A significance level of $\alpha=0.05$ was applied, with *p* values below 0.05 deemed statistically significant.

Results

Macrophage M2 polarization and chemoresistance in GC

Many studies have shown that M2 macrophage polarization is closely related to tumor chemoresistance, but research on exosomes derived from macrophages and their role in tumor resistance is scarce. To test our hypothesis, we induced M2 macrophages (M2-MM) using IL-1/IL-13. Figures 1A and B illustrate the use of flow cytometry to assess surface marker expression in M2-MM cells. In addition, quantitative analysis of relevant markers was performed using PCR. As shown in Fig. 1C, compared with non-activated macrophages, the M2-associated marker Arg1, IL-10 and TGF- β was significantly upregulated ($p < 0.001$), while the M1-associated marker iNOS showed no significant difference ($p > 0.05$). This confirmed the successful induction of M2 macrophages. Next, we co-cultured MFC GC cells with

Table 1 List of primers used for candidate genes

Gene	Forward	Reverse
Arg1	5-CAGAAGAATGGAAGAGTCAG	5-CAGATATGCAGGGAGTCACC
iNOS	5-CTGCAGCACTTGGATCAG GAAC	5-GGAGTAGCCTGTGTGCACCT
TGF- β	5-ATTCTGGCGTTACCTTGG	5-AGCCCTGTATTCCGCTCTCT
IL-10	5-GCCTTATCGAAATGATCCA	5-TGAGGGTCTTCAGCTTCTCAC
PTEN	5-AGCCTCTTGATGTGTGCATT	5-CCATTGGTAGCCAAACGGAAC

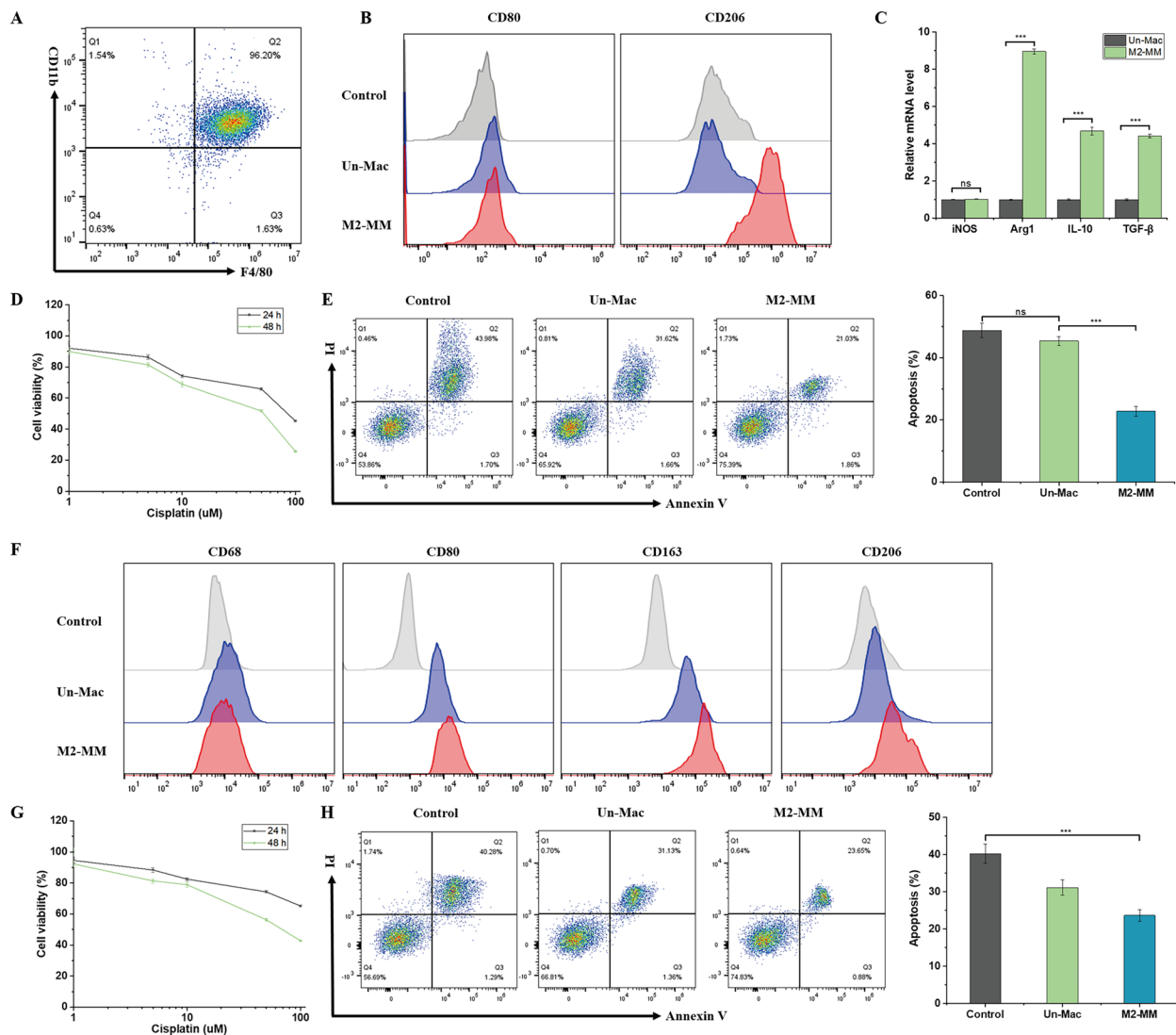


Fig. 1 M2-MM increases DPP resistance in gastric cancer cells. Flow cytometry analysis was performed to examine the expression of M2-MM-associated markers after IL-1/IL-13 induction in the gastric cancer cell line MFC. The following markers were evaluated: **A** M2-MM-associated surface markers F4/80 and CD11b. **B** M1 and M2 macrophage markers, CD80 and CD206. Additionally, the expression of macrophage-related markers was quantified using PCR: **C** PCR analysis of macrophage-associated markers was conducted. To assess the effects of cisplatin (DDP) on gastric cancer cell viability, different concentrations of cisplatin were co-cultured with MFC cells for 24 h and 48 h: **D** the CCK-8 assay was used to evaluate cell viability after co-culture with varying concentrations of DDP and MFC for 24 h and 48 h. The impact of M2-polarized macrophages on apoptosis in gastric cancer cells was further analyzed: **E** flow cytometry was used to analyze apoptosis in MFC cells co-cultured with the respective groups for 24 h, followed by quantitative analysis of apoptotic rates. For human peripheral blood mononuclear cells (PBMCs): **F** flow cytometry was conducted to examine M2-MM marker expression after IL-1/IL-13 induction in PBMCs. Similarly, different concentrations of cisplatin were co-cultured with human gastric cancer cells MGC-803. **G** CCK-8 assay evaluated the cell viability of MGC-803 co-cultured with different concentrations of cisplatin for 24 h and 48 h. Statistical significance is indicated as follows: * $p < 0.05$, ** $p < 0.01$, *** $p < 0.001$ ($N \geq 3$)

different concentrations of DDP for 24 and 48 h and analyzed changes in cell viability. As shown in Fig. 1D, MFC cell viability decreased with increasing concentrations of DDP. To assess if M2-polarized macrophages induce chemoresistance in GC cells, the cells were exposed to DDP for 48 h and subsequently co-cultured with M2-MM using a transwell chamber. The study found

that apoptosis rates were significantly lower in cells co-cultured with M2-polarized macrophages compared to those co-cultured with non-activated macrophages or normal control cells (Fig. 1E). To confirm the effect of M2-MM on GC chemoresistance, we analyzed human peripheral blood mononuclear cells (PBMC) and GC MGC-803 cells. Figure 1F demonstrates the successful

induction of M2 polarization in PBMC using the same method. MGC-803 cells were co-cultured with varying DDP concentrations for 24 and 48 h. As shown in Fig. 1G, MGC-803 cell viability also decreased with increasing concentrations of DDP. Aligned with prior studies, cells co-cultured with M2-MM exhibited notably reduced apoptosis rates compared to those with non-activated macrophages or normal control cells (Fig. 1H). Collectively, these data suggest that M2-polarized macrophages promote DDP resistance in GC cells.

Exosome-mediated chemoresistance in GC

MFC cells were exposed to exosomes isolated from M2 macrophages for 48 h to explore their role in DDP resistance in GC cells. The cells were then co-cultured with 50 µg/mL DDP for 72 h. Figure 2A illustrates that cells co-cultured with M2-exos exhibited significantly higher viability than the control group ($p < 0.01$). Additionally, the apoptosis rate of MFC cells co-treated with

M2-exos was lower than that of cells treated normally (Fig. 2B). The chemoresistance observed in human GC MGC-803 cells (Fig. 2C, D) supports the shared role of M2-exos in both human and mouse models. To investigate the impact of M2-exos on chemoresistance in vivo, MFC cells treated with M2-exos were subcutaneously injected into male nude mice, with subsequent monitoring of tumor volume and weight changes. Figure 2E demonstrates that the DDP group exhibited the slowest tumor volume increase compared to the control group, highlighting DDP's potent antitumor effect. However, the tumor volume in the M2-exo + DDP group increased faster than in the DDP group alone. Furthermore, post-treatment tumor weights were analyzed. Figure 2F and G demonstrate that DDP markedly suppressed tumor growth relative to the control group, whereas M2-exos counteracted this suppression. Overall, the findings indicate that M2-exos can promote DDP resistance in GC cells in both in vitro and in vivo settings.

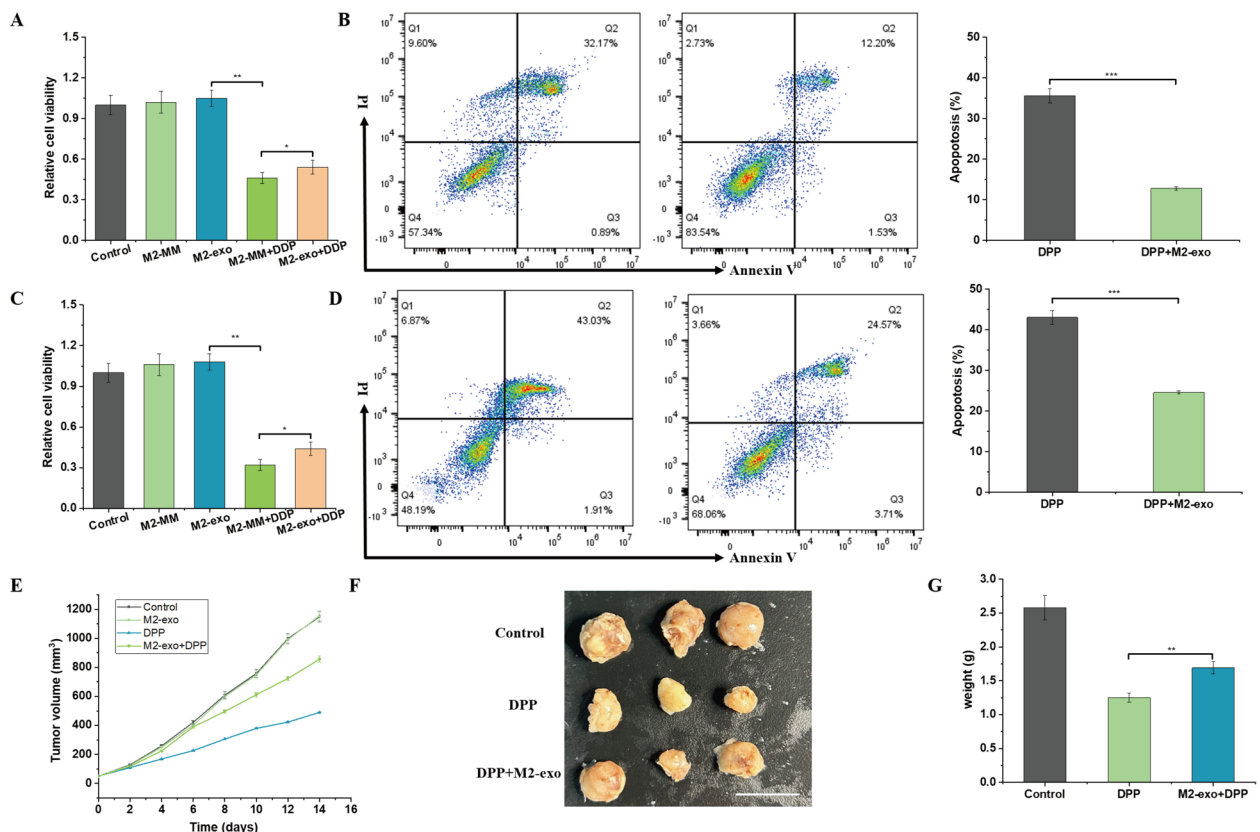


Fig. 2 The impact of M2-exosomes on DDP resistance in gastric cancer cells. **A** Cell viability of the gastric cancer cell line MFC after co-culture with different treatment groups was assessed using the CCK-8 assay. **B** Flow cytometry analysis was conducted to evaluate apoptosis in MFC cells co-cultured with M2-exosomes, followed by a quantitative analysis of apoptotic rates. **C** The effect of co-culture with different treatment groups on the cell viability of human gastric cancer cells MGC-803 was also assessed using the CCK-8 assay. **D** Flow cytometry analysis was performed to evaluate apoptosis in MGC-803 cells co-cultured with M2-exosomes, followed by a quantitative analysis of apoptotic rates. **E** Tumor growth curves were recorded following the subcutaneous injection of tumor cells. After the completion of treatment, the following were assessed: **F** photographs of the tumors. **G** Tumor weights were measured. Statistical significance is indicated as follows: * $p < 0.05$, ** $p < 0.01$, *** $p < 0.001$

Exosome miR-194 and chemoresistance

The role and mechanism of exosome-derived miR-194 in GC resistance remain unexplored in current studies. PCR analysis revealed significantly elevated miR-194 expression in macrophages, particularly in M2-polarized macrophages, compared to MFC cells (Fig. 3A; Fig. S1). M2-exos exhibited elevated miR-194 levels compared to non-activated macrophages. Intracellular miR-194 levels in MFC cells significantly increased following co-culture with M2-polarized macrophages or M2-exos. Confocal microscopy revealed Cy3-labeled signals in GC cells treated with exosomes from Cy3-miR-194 transfected cells, whereas no signals were observed in cells treated with exosomes from mock-transfected macrophages (Fig. 3B). Collectively, these data indicate that exosome-mediated miR-194 shuttling occurs from M2 macrophages to GC cells.

miR-194 decreases chemosensitivity and apoptosis in gastric cancer cells

To determine whether miR-194 induces DDP resistance in GC cells, we directly transfected MFC cells with miR-194 mimics or a negative control and assessed the effect of miR-194 on DDP sensitivity. Figure 4A indicates that cell viability was comparable between the DDP and DDP + miR-NC groups, whereas the miR-194 group exhibited a significant increase in cell viability ($p < 0.001$). Crystal violet staining was used to examine the impact of miR-194 on DDP resistance in MFC cells. Figure 4B illustrates a significant increase in colony count in the miR-194 + DDP group compared to the control group. We further analyzed DDP-induced apoptosis in GC cells transfected with miR-194 mimics or miR-NC using the FITC Annexin V apoptosis detection kit. As shown

in Fig. 4C, apoptosis rates were lower in miR-194-transfected GC cells than in mock-transfected cells. To investigate the role of miR-194 in chemoresistance in vivo, male nude mice were subcutaneously injected with miR-194-transfected MFC cells and subsequently treated with an optimal dose of DDP. MFC cells transfected with miR-NC were used as a negative control. Figure 4D demonstrates that the final tumor size in the miR-194 group exceeded that of the control group, suggesting that miR-194 markedly reduced the chemotherapeutic efficacy of DDP. In conclusion, the findings indicate that miR-194 diminishes chemosensitivity and apoptosis in GC cells.

Exosomal miR-194 modulates the PTEN/PI3K/AKT pathway to enhance anti-apoptotic capacity

In our model, we sought to determine whether exosome-mediated transfer of functional miR-194 also exerts the same effect. We analyzed PI3K/AKT pathway proteins in MFC cells subjected to M2-exos treatment and miR-194 overexpression. Our findings indicate that M2-exos reduce PTEN mRNA and protein levels and enhance AKT phosphorylation (Fig. 5A–C). The data indicate that exosome-mediated transfer of miR-194 contributes to increased chemoresistance in gastric cancer cells by modulating the PTEN/PI3K/AKT signaling pathway. In addition, increasing evidence suggests that resistance to apoptosis contributes to chemoresistance. Previous reports have shown that Bcl-2, a critical anti-apoptotic gene, is directly regulated by miR-194. Therefore, we next examined whether miR-194 affects Bcl-2 expression. Western blot analysis demonstrated that both M2-exos treatment and miR-194 overexpression significantly elevated Bcl-2 protein levels in MFC cells, potentially

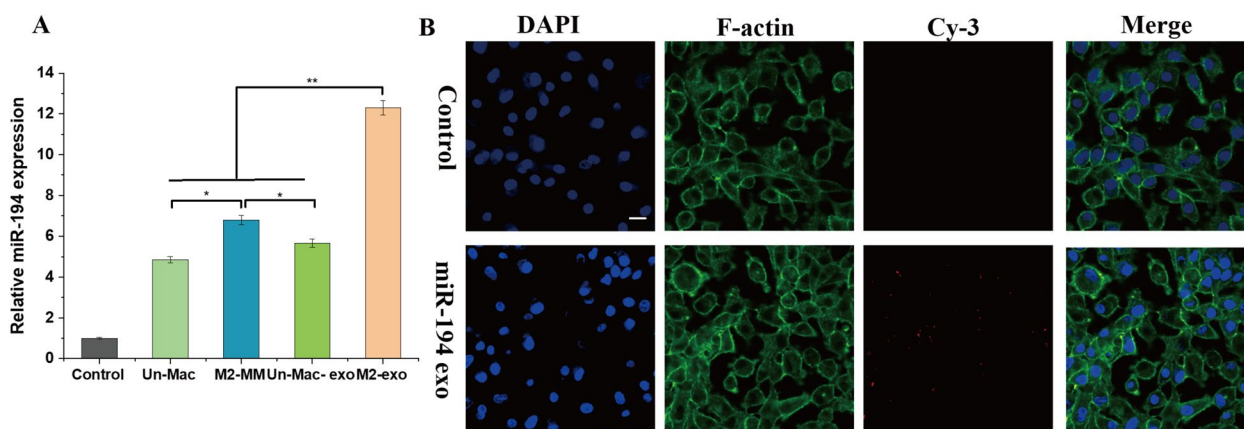


Fig. 3 Transfer of miR-194 exosomes to gastric cancer cells. **A** PCR analysis was conducted to assess the expression levels of miR-194 in the various treatment groups co-cultured with MFC cells. **B** The localization of miR-194 in MFC cells was examined using laser confocal microscopy. Blue: DAPI staining (nuclear marker), Green: Alexa 488 conjugated, Red: miR-194 ($N \geq 3$)

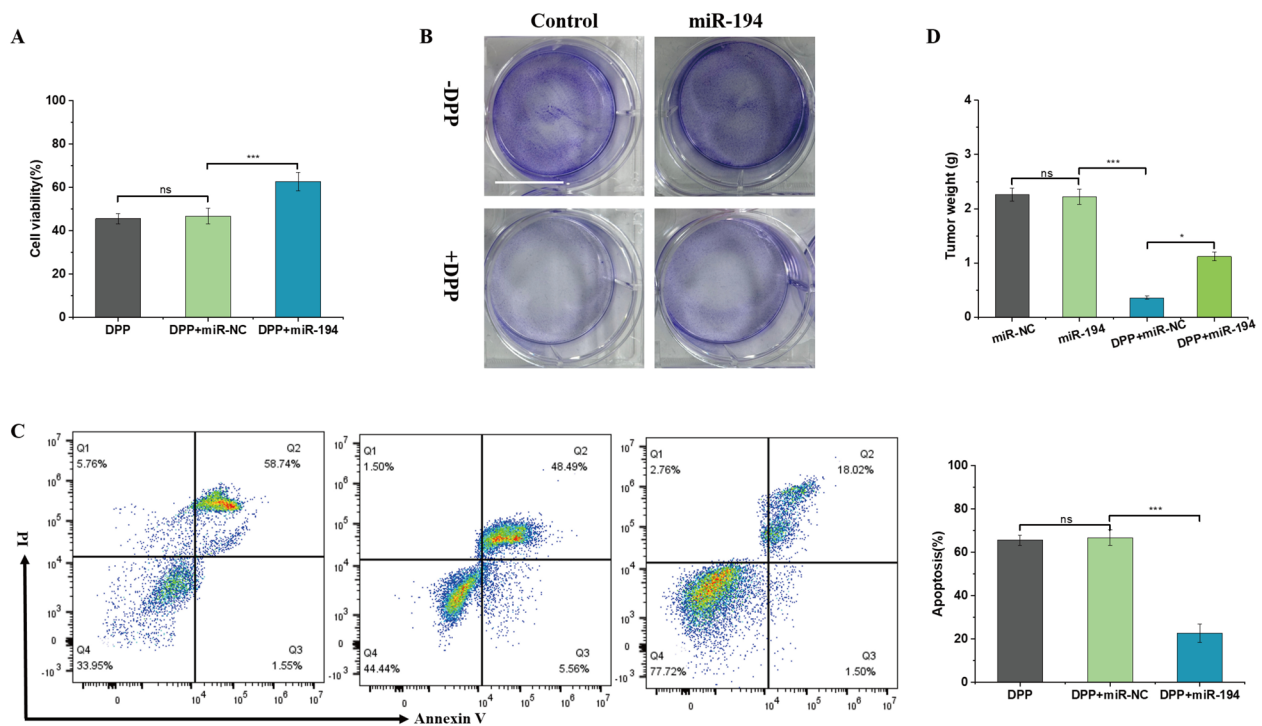


Fig. 4 Impact of miR-194 on DDP resistance in gastric cancer cells. **A** Cell viability after co-culture of MFC cells with different treatment groups was assessed using the CCK-8 assay. **B** Crystal violet staining was employed to visualize the effects of miR-194 on cell colony formation. **C** The effects of different treatment groups on apoptosis in MFC cells were analyzed using flow cytometry, with quantitative analysis presented. **D** Average tumor weights from mice injected with MFC cells transfected with either miR-194 mimic or miR-NC are shown. Statistical significance is indicated as follows: * $p < 0.05$, ** $p < 0.01$, *** $p < 0.001$ ($N \geq 3$)

contributing to increased anti-apoptotic capacity (Fig. 5D–F).

Discussion

Currently, cisplatin remains a cornerstone chemotherapeutic agent for treating GC, but resistance to cisplatin-based chemotherapy diminishes its efficacy in some tumor patients [16]. Research has shown that multiple molecular mechanisms contribute to cisplatin resistance in gastric cancer cells [17]. Mechanisms such as increased detoxification through altered glutathione transferase and metallothionein levels, along with heightened activity of cell membrane drug efflux pumps like P-glycoprotein, BCRP, and multidrug resistance proteins, lower the intracellular concentration of toxic drugs [17]. Other mechanisms include enhanced DNA repair capabilities and defective or inhibited apoptosis-related pathways. However, the exact mechanisms behind cisplatin resistance in GC remain unclear [18]. Therefore, further exploration of the mechanisms driving cisplatin resistance and identifying molecular targets to reverse this resistance holds significant clinical value in overcoming chemotherapy challenges in GC patients.

Macrophages, known as tumor-associated macrophages (TAMs), are essential stromal cells within the tumor microenvironment. Tumor-associated macrophages (TAMs) are diverse, including M2 macrophages that facilitate tumor growth and M1 macrophages that suppress tumor progression. The tumor microenvironment is typically enriched with factors that favor the differentiation of M2 macrophages. M2 macrophages significantly contribute to tumor growth, invasion, and metastasis in various cancers. Research by Dijkgraaf et al. [19] has shown that TAMs are closely linked to tumor cell chemoresistance, with chemotherapy inducing the differentiation of macrophages into M2 macrophages that further enhance the resistance of tumor cells to chemotherapeutic agents.

Exosomes, crucial for intercellular communication, significantly influence tumorigenesis, growth, invasion, metastasis, and drug resistance [20]. Recent studies have shown that exosomes influence drug resistance in target cells by transferring proteins or microRNAs (miRNAs). For example, Xiao et al. [21] showed that cisplatin treatment increased exosome secretion in the lung adenocarcinoma cell line A549, with a significant elevation in exosomal miR-21 and miR-133

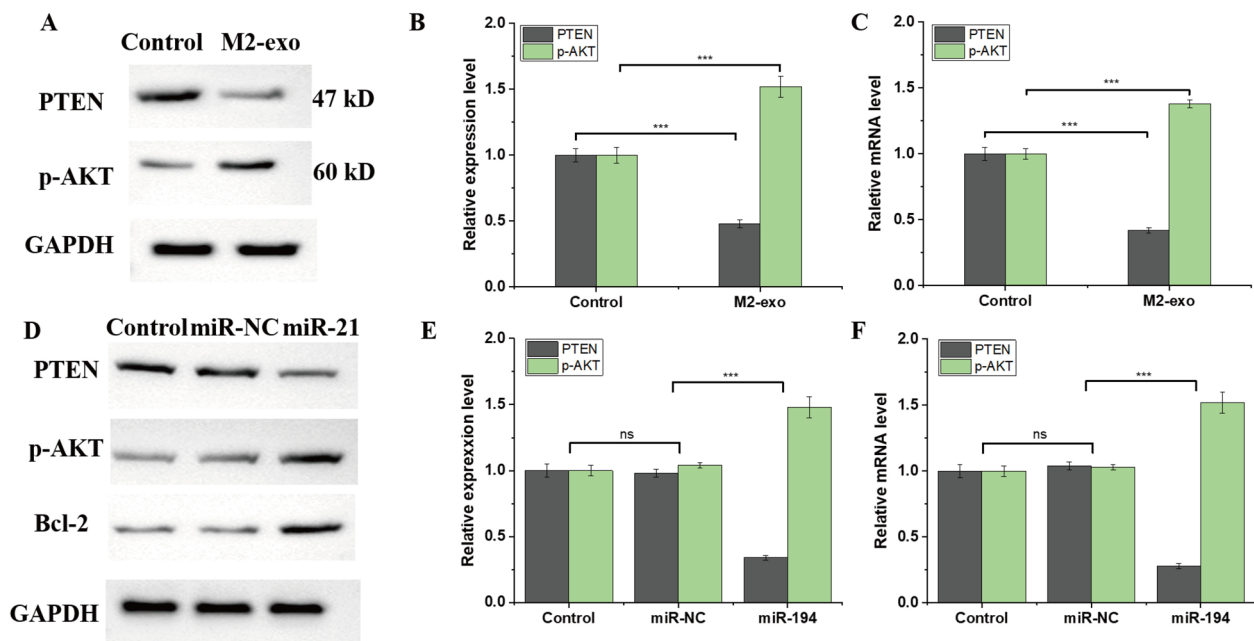


Fig. 5 Regulation of DDP resistance in gastric cancer cells by miR-194 through the PTEN/AKT signaling pathway. **A** WB analysis was conducted to evaluate the expression levels of PTEN and phosphorylated AKT (p-AKT) in gastric cancer cells co-cultured with M2-exosomes (M2-exo). **B** Quantitative analysis of PTEN and p-AKT expression levels, showing the impact of M2-exo on these signaling proteins. **C** PCR analysis confirmed the expression levels of PTEN and p-AKT in gastric cancer cells after co-culture with M2-exo. **D** Another set of WB analysis reiterating the effects of M2-exo on PTEN and p-AKT expression levels. **E** Quantitative analysis of PTEN, p-AKT and Bcl-2 expression levels. **F** PCR analysis confirmed the expression levels of PTEN and p-AKT in gastric cancer cells after co-culture with miR-21. Statistical significance is indicated as follows: * $p < 0.05$, ** $p < 0.01$, *** $p < 0.001$ ($N \geq 3$)

levels. Transferring these miRNA-rich exosomes to sensitive cells markedly enhanced their resistance to cisplatin. Similarly, exosomes enriched with miR-155 from monocytes have been shown to increase cisplatin resistance in neuroblastoma cells [22]. This study demonstrates that exosomes from M2-polarized macrophages can induce DDP resistance in GC cells in vitro and in vivo, indicating that tumor-associated macrophages may enhance GC invasiveness via exosome secretion.

Our data demonstrate that exosomal miR-194 derived from tumor-associated macrophages reduces GC cell sensitivity to chemotherapy and inhibits apoptosis. This discovery offers fresh perspectives on the mechanisms underlying drug resistance in GC. Additionally, we investigated how miR-194 enhances DDP resistance in GC cells. MiR-194 influences tumor cell malignancy via the PTEN/PI3K/AKT signaling pathway across multiple cancer types, including gastric cancer [23].

In summary, our findings suggest that targeting exosome-mediated miRNA transfer, particularly miR-194, may represent a promising strategy for overcoming chemoresistance in GC. Understanding the role of exosomes and their miRNA cargo in drug resistance could open new avenues for developing therapeutic

interventions aimed at enhancing the efficacy of chemotherapy in GC patients.

Supplementary Information

The online version contains supplementary material available at <https://doi.org/10.1186/s40001-025-02329-5>.

Additional file 1. Figure S1: The top 10 most abundant miRNAs in M2-Exo.

Additional file 2.

Acknowledgements

Not applicable.

Author contributions

Y.Z. conducted the majority of the experiments and wrote the manuscript and Y.S. contributed to the experimental design and data analysis and Y.Z. assisted in the cell culture and exosome isolation procedures and J.W. was responsible for the statistical analysis of the data and X.Z. helped with the interpretation of the results and manuscript revision and X.S. supervised the project and provided critical feedback on the manuscript. All authors reviewed the manuscript.

Funding

This study has received no funding support.

Availability of data and materials

No datasets were generated or analysed during the current study. Data is available from the corresponding author on reasonable request.

Declarations

Ethical approval and consent to participate

The animal study was conducted in accordance with the ethical standards and guidelines set forth by the Ethics Committee of The Experimental Animal Welfare Ethics Committee of Zhongda Hospital, School of Medicine, Southeast University. The study protocol was reviewed and approved by the Ethics Committee, with the permit number: 20220926001. Procedures involving animals and their care were conducted in conformity with NIH guidelines (NIH Pub. No. 85-23, revised 1996). The maximal tumor size permitted by our institutional ethics committee guidelines is 2 cm in diameter, or any tumor burden that does not cause significant discomfort, impaired mobility, or affect the well-being of the animal. We confirm that the maximal tumor size/burden as outlined by our ethics committee was not exceeded at any point during the study. In all cases, animals were closely monitored, and any discomfort or significant tumor growth was addressed promptly. In instances where tumors approached the size limit, animals were euthanized following the approved humane endpoints to avoid exceeding the permitted tumor burden. In addition, the research protocol for this study was rigorously reviewed and approved by the Medical Ethics Committee of Wuzhong People's Hospital, under the approval number 2024lw03. This endorsement signifies adherence to ethical standards and guidelines for conducting research involving human participants. Prior to participation, all patients involved in this study were fully informed about the nature and objectives of the research. Written informed consent was obtained from each participant, ensuring their voluntary engagement and comprehension of the research procedures and implications.

Consent for publication

Every patient participant had been aware of this research and provided their consent.

Competing interests

The authors declare no competing interests.

Received: 3 November 2024 Accepted: 23 January 2025

Published online: 04 February 2025

References

- Wang Y, Zhang L, Tan J, Zhang Z, Liu Y, Hu X, Lu B, Gao Y, Tong L, Liu Z, et al. Longitudinal detection of subcategorized CD44v6⁺ CTCs and circulating tumor endothelial cells (CTECs) enables novel clinical stratification and improves prognostic prediction of small cell lung cancer: a prospective, multi-center study. *Cancer Lett.* 2023;571: 216337. <https://doi.org/10.1016/j.canlet.2023.216337>.
- Andreucci E, Biagioni A, Peri S, Versienti G, Cianchi F, Staderini F, Antonuzzo L, Supuran CT, Olivo E, Pasqualini E, et al. The CAIX inhibitor SLC-0111 exerts anti-cancer activity on gastric cancer cell lines and resensitizes resistant cells to 5-fluorouracil, taxane-derived, and platinum-based drugs. *Cancer Lett.* 2023;571: 216338. <https://doi.org/10.1016/j.canlet.2023.216338>.
- Zhou S, Zheng J, Zhai W, Chen Y. Spatio-temporal heterogeneity in cancer evolution and tumor microenvironment of renal cell carcinoma with tumor thrombus. *Cancer Lett.* 2023;572: 216350. <https://doi.org/10.1016/j.canlet.2023.216350>.
- Salati M, Orsi G, Smyth E, Aprile G, Beretta G, De Vita F, Di Bartolomeo M, Fanotto V, Lonardi S, Morano F, et al. Gastric cancer: translating novel concepts into clinical practice. *Cancer Treat Rev.* 2019;79: 101889. <https://doi.org/10.1016/j.ctrv.2019.101889>.
- Su H, Yuan Y, Tang J, Zhang Y, Wu H, Zhang Y, Liang J, Wang L, Zou X, Huang S, et al. The ATR inhibitor VE-821 increases the sensitivity of gastric cancer cells to cisplatin. *Transl Oncol.* 2023;36: 101743. <https://doi.org/10.1016/j.tranon.2023.101743>.
- Zhu F, He X, Shuang F, Fang X, Jiang J. Wnt/ β -catenin signaling activation by TIMP1 confers cisplatin-resistant gastric cancer cells to malignant behaviors and epithelial-mesenchymal transition. *Oncologie.* 2023;25(2):169–78. <https://doi.org/10.1515/oncologie-2022-1028>.
- Zheng P, Chen L, Yuan X, Luo Q, Liu Y, Xie G, Ma Y, Shen L. Exosomal transfer of tumor-associated macrophage-derived miR-21 confers cisplatin resistance in gastric cancer cells. *J Exp Clin Cancer Res.* 2017;36(1):53. <https://doi.org/10.1186/s13046-017-0528-y>.
- Laurino S, Brancaccio M, Angrisano T, Calice G, Russi S, Mazzone P, Di Paola G, Aieta M, Grieco V, Bianchino G, et al. Role of IL-6/STAT3 axis in resistance to cisplatin in gastric cancers. *Biomedicines.* 2023;11(3):694. <https://doi.org/10.3390/biomedicines11030694>.
- Gao Z, Qi N, Qin X, Li Z, Li G, Wang Z, Wang J, Wen R, Li H. The addition of tislelizumab to gemcitabine and cisplatin chemotherapy increases thrombocytopenia in patients with urothelial carcinoma: a single-center study based on propensity score matching. *Cancer Med.* 2023;12(24):2071–80. <https://doi.org/10.1002/cam4.6807>.
- Xia K, Wang Z, Liu B, Wang W, Liu Y, Tang J, Yan J. Functions of circular RNAs and their potential applications in gastric cancer (Review). *Oncol Lett.* 2023;25(6):217. <https://doi.org/10.3892/ol.2023.13803>.
- Ebrahimi N, Hakimzadeh A, Bozorgmand F, Speed S, Manavi MS, Khorram R, Farahani K, Rezaei-Tazangi F, Mansouri A, Hamblin MR, et al. Role of non-coding RNAs as new therapeutic targets in regulating the EMT and apoptosis in metastatic gastric and colorectal cancers. *Cell Cycle.* 2023;22(20):2302–23. <https://doi.org/10.1080/15384101.2023.2286804>.
- Yamaguchi T, Takashima A, Nagashima K, Kumagai K, Yamada T, Terashima M, Yabusaki H, Nishikawa K, Tanabe K, Yunome G, et al. Evaluating the efficacy of post-operative chemotherapy after curative resection of stage IV gastric cancer with synchronous oligo metastasis: a multicenter retrospective study. *Gastric Cancer.* 2023;26(2):307–16. <https://doi.org/10.1007/s10120-023-01363-8>.
- Fu Q, Wu X, Lu Z, Chang Y, Jin Q, Jin T, Zhang M. TMEM205 induces TAM/M2 polarization to promote cisplatin resistance in gastric cancer. *Gastric Cancer.* 2024;27(5):998–1015. <https://doi.org/10.1007/s10120-024-01517-2>.
- Wang H, Liu M, Zeng X, Zheng Y, Wang Y, Zhou Y. Cell death affecting the progression of gastric cancer. *Cell Death Discov.* 2022;8(1):377. <https://doi.org/10.1038/s41420-022-01161-8>.
- Song H, Weinstein HN, Allegakoen P, Wadsworth MH II, Xie J, Yang H, Castro EA, Lu KL, Stohr BA, Feng FY, et al. Single-cell analysis of human primary prostate cancer reveals the heterogeneity of tumor-associated epithelial cell states. *Nat Commun.* 2022;13(1):141. <https://doi.org/10.1038/s41467-021-27322-4>.
- Lee H, Horbath A, Kondiparthi L, Meena JK, Lei G, Dasgupta S, Liu X, Zhuang L, Koppula P, Li M, et al. Cell cycle arrest induces lipid droplet formation and confers ferroptosis resistance. *Nat Commun.* 2024;15(1):79. <https://doi.org/10.1038/s41467-023-44412-7>.
- Niu L, Li Y, Huang G, Huang W, Fu J, Feng L. FAM120A deficiency improves resistance to cisplatin in gastric cancer by promoting ferroptosis. *Commun Biol.* 2024;7(1):399. <https://doi.org/10.1038/s42003-024-06097-6>.
- Wang J, Liang W, Wang X, Chen Z, Jiang L. LTBP2 regulates cisplatin resistance in GC cells via activation of the NF- κ B2/BCL3 pathway. *Genet Mol Biol.* 2024;47(2): e20230231. <https://doi.org/10.1590/1678-4685-GMB-2023-0231>.
- Dijkgraaf EM, Heusinkveld M, Tummers B, Vogelpoel LTC, Goedemans R, Jha V, et al. Chemotherapy alters monocyte differentiation to favor generation of cancer-supporting m2 macrophages in the tumor microenvironment. *Cancer Res.* 2013;73(8):2480–92. <https://doi.org/10.1158/0008-5472.CAN-12-3542>.
- Zhang Y, Fan A, Li Y, Liu Z, Yu L, Guo J, Hou J, Li X, Chen W. Single-cell RNA sequencing reveals that HSD17B2 in cancer-associated fibroblasts promotes the development and progression of castration-resistant prostate cancer. *Cancer Lett.* 2023;566: 216244. <https://doi.org/10.1016/j.canlet.2023.216244>.
- Xiao X, Yu S, Li S, Wu J, Ma R, Cao H, et al. Exosomes: decreased sensitivity of lung cancer a549 cells to cisplatin. *PLoS One.* 2014;9(2):e89534. <https://doi.org/10.1371/journal.pone.0089534>.
- Wu CY, Shu LH, Liu HT, Cheng YC, Wu YH, Wu YH. The role of MRE11 in the IL-6/STAT3 pathway of lung cancer cells. *Curr Issues Mol Biol.* 2022;44(12):6132–44. <https://doi.org/10.3390/cimb44120418>.
- Yuan L, Wei H, Pan Z, Deng X, Yang L, Wang Y, Lu D, Li Z, Luo F, Li J, et al. A bioinspired injectable antioxidant hydrogel for prevention of postoperative adhesion. *Journal of Materials Chemistry B.* 2024;12(28):6968–80. <https://doi.org/10.1039/d4tb00805g>.

Publisher's Note

Springer Nature remains neutral with regard to jurisdictional claims in published maps and institutional affiliations.